A First-Principles Analysis of Acetylene Hydrogenation over Pd(111)

Priyam A. Sheth,[†] Matthew Neurock,*[,†] and C. Michael Smith[‡]

Department of Chemical Engineering, University of Virginia, Charlottesville, Virginia 22904-4741, and The Dow Chemical Company, Freeport, Texas 77541-3257

Received: June 5, 2002; In Final Form: December 9, 2002

Nonlocal gradient-corrected periodic density functional theory (DFT) calculations have been carried out to examine the hydrogenation of acetylene over Pd(111). The binding energies of acetylene, atomic hydrogen, vinyl, and ethylene at 25% (33%) coverage were computed to be −172 (−136), −260 (−248), −274 (−235), and −82 (−62) kJ/mol, respectively. The reaction energy for acetylene hydrogenation to vinyl over Pd(111) was found to be −26 (−43) kJ/mol at 25% (33%) coverage. The overall reaction energy for vinyl hydrogenation to ethylene was calculated to be −58 and −73[1] kJ/mol at 25% and 33% coverages, respectively. Acetylene hydrogenation to vinyl is therefore less exothermic than vinyl hydrogenation to ethylene. The intrinsic activation barrier for the addition of atomic hydrogen to acetylene over Pd was calculated to be +66 kJ/mol at 25% coverage and +50 kJ/mol at 33% coverage. The barrier for vinyl hydrogenation to form ethylene over Pd(111) at 25% coverage was computed at +85 kJ/mol while that at 33% coverage[1] was found to be +78 kJ/mol. Higher pressures of hydrogen can also lead to the formation of surface Pd hydride phases that could alter the hydrogenation kinetics. Initial results for Pd(111) with a 2 × 2 subsurface layer of hydrogen, indicate that there are moderate changes in the adsorption energies due to the presence of subsurface hydrogen. The changes in the overall reaction energies and activation barriers, however, are less than 3 kJ/mol. The activation barrier for hydrogen to diffuse from the subsurface was calculated to be +58 kJ/mol.

Introduction

The production of high purity ethylene feeds for olefin polymerization and copolymerization processes requires the selective hydrogenation of acetylene impurities from crude ethylene feedstocks. Supported palladium is unique in its ability to selectively hydrogenate ppm levels of acetylene from these ethylene feeds. Silver or gold are typically alloyed with palladium in order to control the reaction selectivity.[2−4] Catalytic hydrogenation, however, is quite sensitive to the actual operating conditions.[5] There is a narrow window in which acetylene can be selectively hydrogenated to ethylene without undergoing over-hydrogenation of ethylene to ethane. The overall reaction of ethylene to ethane is fairly exothermic at 137 kJ/mol.[6] Any uncontrolled increases in temperature will enhance the rate of ethylene hydrogenation and further raise temperature. This creates the potential for runaway reactions. A number of studies have therefore been directed at understanding the factors that influence the selectivity differences that arise between acetylene and ethylene hydrogenation.

In general, the overall reaction paths for the hydrogenation of acetylene are thought to follow a Horuiti-Polanyi[7] scheme where a sequence of hydrogenated C_2H_x species are formed by the sequential addition of single hydrogen atoms to the adsorbed hydrocarbon intermediate (Scheme 1).

This reaction scheme was initially suggested by Bond and Wells who used deuterium labeling to follow the kinetics of acetylene hydrogenation over different transition metals.[8−11] Their results for acetylene hydrogenation over Pd/Al_2O_3[12] identified the doubly deuterated ethylene intermediate (ethylene-d_2) to be the major product formed. Other deuterated isomers such as ethylene-d_1 and ethylene-d_3 were also observed in small amounts. Further infrared analysis on the total yield of the ethylene-d_2 formed revealed that 74% of the isomer formed was *cis*-ethylene-d_2. The trans isomer was found to be present at 15% while the asymmetric isomer was found to be present at 10% (Scheme 2). Studies by Arnett and Crawford[13] also reported the formation of all three deuterated isomers in agreement with the results by Bond and Wells. These results therefore suggest that the hydrogenation likely proceeds through a series of successive hydrogenation addition steps rather than simultaneous hydrogenation steps. The direct hydrogenation of acetylene to ethane was also shown to be negligible over Pd.[14]

These early conclusions on the reaction mechanism led to a series of thermodynamic explanations as to why Pd was selective toward ethylene formation.[15] It was thought that the strongly

SCHEME 1

$C_2H_2(g) + * \longleftrightarrow C_2H_2*$

$H_2(g) + 2* \longleftrightarrow 2H*$

$C_2H_2* + H* \longleftrightarrow C_2H_3* + *$

$C_2H_3* + H* \longrightarrow C_2H_4* + *$

$C_2H_4* \longrightarrow C_2H_4(g) + *$

$C_2H_2(g) + H_2(g) \Rightarrow C_2H_4(g)$ *(overall reaction)*

SCHEME 2

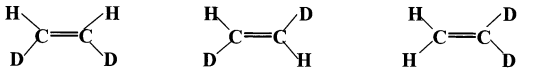

* Author to whom correspondence should be addressed.
[†] University of Virginia.
[‡] The Dow Chemical Company.

10.1021/jp021342p CCC: $25.00
Published on Web 02/11/2003

bound acetylene species displaced the more weakly bound ethylene from the Pd surface. The surface would therefore be predominantly covered with acetylene. The rate of acetylene hydrogenation is therefore thought to be significantly faster than that for ethylene hydrogenation. McGown et al.[16] later established, however, that this argument was insufficient, as it could not explain the small but significant ethylene hydrogenation observed under high acetylene partial pressures. The presence of other carbonaceous intermediates on the surface was also not accounted for by these classical thermodynamic arguments. Subsequent explanations have been proposed to account for the deviations from this classical thermodynamic picture. They suggest that there may be more than one active site and that the intermolecular competition for adsorption at each site may be different. Incorporating these ideas into a description of the kinetics of acetylene hydrogenation leads to the development of much more complex rate expressions.[16−21]

A number of kinetic models have been developed over the past thirty years to describe the overall kinetics along with specific features concerning the mechanism. Bos and Westerterp[6,22] provide a nice review of many of these models and probe the validity of these models by comparing their results with a sufficiently large experimental data set. The results from these studies suggest that the reaction order for hydrogen is 1 to 1.5 and the order for acetylene is 0 to −0.5 on the overall rate of acetylene hydrogenation. These rate equations, however, are typically applicable only under a narrow range of operating conditions[6] to which they have been parametrized. While these models provide a useful starting point, they average over many of the important local surface features and their tie to the fundamental elementary steps is qualitative at best.

Many of the important physicochemical steps involved in the selective and unselective paths for acetylene hydrogenation have been analyzed under more ideal conditions in order to provide fundamental explanations of the elementary steps that take place and the role of the atomic surface structure. A wealth of information on the adsorption and subsequent reactivity of acetylene and ethylene on metal surfaces already exists from experimental surface science as well as theoretical studies that have been reported in the literature. We discuss here only the current thinking regarding some of the basic elementary steps important for acetylene hydrogenation over Pd, including acetylene adsorption, coadsorption of acetylene and hydrogen, ethylene adsorption, and the hydrogenation of acetylene and ethylene.

Scanning tunneling microscopy (STM) studies reported by Jannsens indicate that acetylene adsorbs on Pd(111) and forms two ordered phases as seen by the 2×2 and $\sqrt{3} \times \sqrt{3}$ R30 LEED pattern at 140 K under UHV conditions.[23] Further work by Dunphy et al.[24,25] indicates that acetylene prefers to sit at both the fcc and hcp hollow sites on Pd(111). At 44 K the rotation of these molecules was found to be quite facile at these sites. Diffusion of acetylene at 44 K, however, was found to be slow but increases significantly with increases in temperature. First principle calculations were carried out to help interpret these STM observations. The results showed that the parallel configurations of acetylene are favored over Pd rather than the perpendicular orientations, which agrees with experiment. The calculations predict that acetylene is strongly bound at both of these hollow sites with adsorption energies (145−136 meV) which is in good agreement with observed values of 113 meV from experiment. The resulting electron densities for acetylene on Pd were subsequently also incorporated into an electron scattering quantum chemistry algorithm[24] (ESQC) in order to simulate STM images. These calculated images were found to be in good agreement with the experimental STM images.

Theory has also been used to understand the electronic features that govern the adsorption of acetylene over different metals.[25,26] DFT studies[26,27] on the adsorption of acetylene on nickel, copper, and palladium follow the classical Dewar-Chatt-Duncansan bonding.[28,29] The mechanism involves both electron donation from the occupied acetylene orbitals to the empty surface d-state and electron back-donation from the occupied surface d orbitals into the π^* orbitals of acetylene. These ideas on charge transfer also help to explain the observed distortions in the adsorption geometries of acetylene over the different surfaces.

A number of studies have also been carried out whereby both acetylene and hydrogen are coadsorbed to determine their interactions at low temperature and their potential reaction pathways over Pd as the temperature is increased. Sandell et al.[30] for example, used core-level photoemission spectroscopy to study the coadsorption of acetylene and hydrogen on Pd(111). They report that a well-defined overlayer is not able to form when acetylene is adsorbed above 200 K. At temperatures of 300 K, however, Guo and Madix[31] found that unlike ethylene, which only undergoes H−D exhange, acetylene hydrogenates to ethylene. Furthermore, preadsorbing hydrogen on the Pd(111) surface changes the sticking probability of acetylene depending on the temperature of preadsorption. Upon heating this surface, ethylidyne forms in a $\sqrt{3} \times \sqrt{3}$ R30 structure as demonstrated by LEED. At higher temperatures, ethylidyne decomposes to form carbonaceous deposits on the surface. This is consistent with the work of Tysoe[32] and Kesmodal.[33] A second surface intermediate is also observed to form within the range of 250−270 K. It has not been possible to resolve this intermediate, however, as it coincides within the same range of temperatures for ethylene desorption. Both Tysoe[34] and Gates[35] initially speculated that the intermediate is surface vinylidene. Ab initio calculations performed by Clotet et al.[36] indicate that vinylidene is energetically more favorable than acetylene over Pd(111). Vinylidene was therefore thought to be a possible precursor to ethylene formation and reaction mechanisms considering a vinylidene surface intermediate were thus proposed. Azad et al.[37] and Ormerod et al.[38] however, found that vinylidene is observed only at high temperatures ($T > 300$ K) and is unreactive at UHV conditions. At higher acetylene pressures however, vinylidene reacts with acetylene to form benzene.[39,40] This has therefore led to a reevaluation of the proposed reaction pathways similar to the original Horuiti-Polanyi scheme involving the (spectroscopically) elusive vinyl intermediate. In this proposed reaction pathway, acetylene is first hydrogenated to vinyl. This surface vinyl intermediate can then subsequently react with a second hydrogen atom to form ethylene as proposed by the Horuiti-Polanyi mechanism. In addition to these elementary reaction steps, vinyl can also react to form vinylidene and ethylidyne. Which of these species actually forms will likely depend on the reaction conditions and the active site. And even though vinyl is not observed experimentally, its formation is still thought to be the rate-limiting step for these reactions.[37]

Ethylene adsorption and its subsequent hydrogenation have also been the topic of many surface science and theoretical studies.[11,15,41,42] Ethylene is reported to adsorb on Pd in either of three configurations: di-σ, π, or physisorbed. Hydrogenation of ethylene also proceeds through the Horuiti-Polanyi mechanism in that it is successively hydrogenated to ethane. Ethylene has also been extensively examined using theory as it serves as

a model for olefins as well as aromatics.[42,43−45] We therefore refer the reader to the above references for more detailed information on ethylene hydrogenation.

There have been relatively few ab initio efforts aimed at establishing the kinetics for acetylene hydrogenation over Pd. Nakatsuji et al.[46] performed some of the first ab initio calculations to help confirm that the reaction favors the Langmuir−Hinshelwood mechanism shown in Scheme 1. In this mechanism, acetylene is sequentially hydrogenated to ethylene via a vinyl intermediate. These studies, however, were carried out over small clusters. In addition, the influence of coverage and competing reaction pathways were not studied. In this paper, we examine the adsorption and hydrogenation of acetylene to ethylene at different coverages over Pd(111) using periodic DFT calculations. Intrinsic activation barriers for acetylene and vinyl hydrogenation as well as lateral interaction effects are also reported herein. We also explore the effect of coverage (of the adsorbates) as well as the influence of the α-hydride phase of Pd on the hydrogenation kinetics.

Computational Details

The accuracy of density functional theoretical methods for the prediction of binding and adsorption energies is typically within 5−8 kcal/mol of the reported experimental values.[42,47−49] Much less is known about the activation energies, but they too appear to fall within this range. This is not within the 1 kcal/mol accuracy that might be necessary for engineering models. The predictions, however, are quite useful in that they typically provide the correct trends, even when the energy differences are relatively small. While we expect that there will be some deviations from the exact quantitative accuracy of the results reported herein, the comparison of binding energies, and overall reaction energies and activation barriers for different steps should be fairly reliable.

In addition, it is important to point out that the results reported herein are based only on the electronic energies. A more accurate calculation of the enthalpy requires the calculation of zero-point energy corrections as well as changes in the specific heat in going from 0 K to the specified reference temperature.

The calculations reported here were performed using plane wave periodic density functional theoretical calculations as implemented in the Vienna ab initio Simulation Program (VASP).[50] The interactions between the ions and the electrons were described by Vanderbilt ultrasoft pseudopotentials[51] using a cut-off energy of 286.7 eV. Non local gradient corrections to energy were calculated by using the Perdew-Wang 91 (PW91) exchange correlation potential.[52] PW91 is known to typically overestimate the adsorption energies. The Kohn Sham equations were solved self-consistently by using an iterative matrix diagonalization scheme. The electron density was converged using a self-consistent field approach and the SCF energy is optimized to within a tolerance of 1×10^{-3} eV. A Monkhorst pack scheme was used to generate the k-point grid. Various k-point meshes were examined for these calculations. A $5 \times 5 \times 1$ grid was found to be accurate as well as computationally efficient. Moving from a $5 \times 5 \times 1$ to a $7 \times 7 \times 1$ grid led to changes in energies that were smaller than 0.01 eV. The time required for convergence, however, was significantly longer for the $7 \times 7 \times 1$ grid. All calculations were therefore performed using the $5 \times 5 \times 1$ grid.

The Pd(111) surface was modeled using both $\sqrt{3} \times \sqrt{3}$ and 2×2 super cells. The metal slab was chosen to be three layers thick. A 10 Å vacuum layer was used to ensure that there were no interactions between the surface adsorbates of one layer and the next slab. The top two metal layers along with the adsorbates were allowed to relax in order to relax the surface structure. The bottom layer was held fixed at the bulk positions of palladium. Subsequent calculations using four metal layers showed that the adsorption energy changed by less than 5 kJ/mol. Three metal layers were therefore used to model the surface.

SCHEME 3

A(g) + * ⟶	A*	ΔE = x kJ/mol	*(adsorption)*
B(g) + * ⟶	B*	ΔE = y kJ/mol	*(adsorption)*
C* ⟶	C(g) + *	ΔE = z kJ/mol	*(desorption)*
C(g) ⟶	A(g) + B(g)	ΔE = p kJ/mol	*(gas phase reaction)*
C* +2* ⟶	A* + B* + *	$\Delta E_{overall}$ = (x + y + z + p) kJ/mol *(net reaction energy)*	

Transition states were isolated using the nudged elastic band approach.[53] In this method, a linear path between the reactant and the product states is established as the initial search coordinate. The path is subsequently divided into a series of different images. Each of these images is optimized with respect to all nuclear degrees of freedom except that of the reaction pathway. All forces for a specific image except that which is tangential to the reaction path are minimized to zero. The transition state refers to the image whereby the tangential force to the reaction path goes to zero. From transition state theory,[54] the difference in the energy of the transition state and that of the reactant state is the activation energy.

Conventions

The surface coverages reported herein are given in terms of the hydrocarbon coverage only. In the case of coadsorbed hydrocarbon and hydrogen species, the total surface coverage would actually be higher due to the presence of hydrogen.

The binding (or adsorption) energy of an adsorbate is defined here as the difference in the energy between the adsorbed system (adsorbate and surface) and the base energies of the gas-phase adsorbate and the clean metal slab.

$$\Delta E_{\epsilon} = E_{\text{adsorbed system}} - (E_{\text{adsorbate}} + E_{\text{metal slab}}) \qquad (1)$$

The overall reaction energy for a particular step is calculated in two ways. The first method isolates individual reactant or product species and calculates the ideal reaction energy by constructing a Haber cycle according to Scheme 3. The calculated adsorption energies of the reactants and products along with the gas-phase reaction energy can be used to calculate the surface reaction energy. According to this scheme we isolate coadsorbed reactants (or products) thus removing any interactions the two have on one another. The second method evaluates the reaction energy by explicitly optimizing both the reactant (or both product) species in the same unit cell. As such, it includes the lateral interactions that exist between coadsorbates in either the reactant or product states. Both methods then take the difference in the energies between the product and reactant states as the energy of reaction. This can be expressed as follows:

$$\Delta E_{\text{rxn}} = E_{\text{product}} - E_{\text{reactant}} \qquad (2)$$

As per these conventions a negative value for the reaction energy or adsorption energy indicates that the step is exothermic and releases heat. The calculated energies here refer only to the change of the electronic energy. While this provides an estimate of the overall heat of reaction, the actual heat of reaction would require the calculation of zero-point energies along with

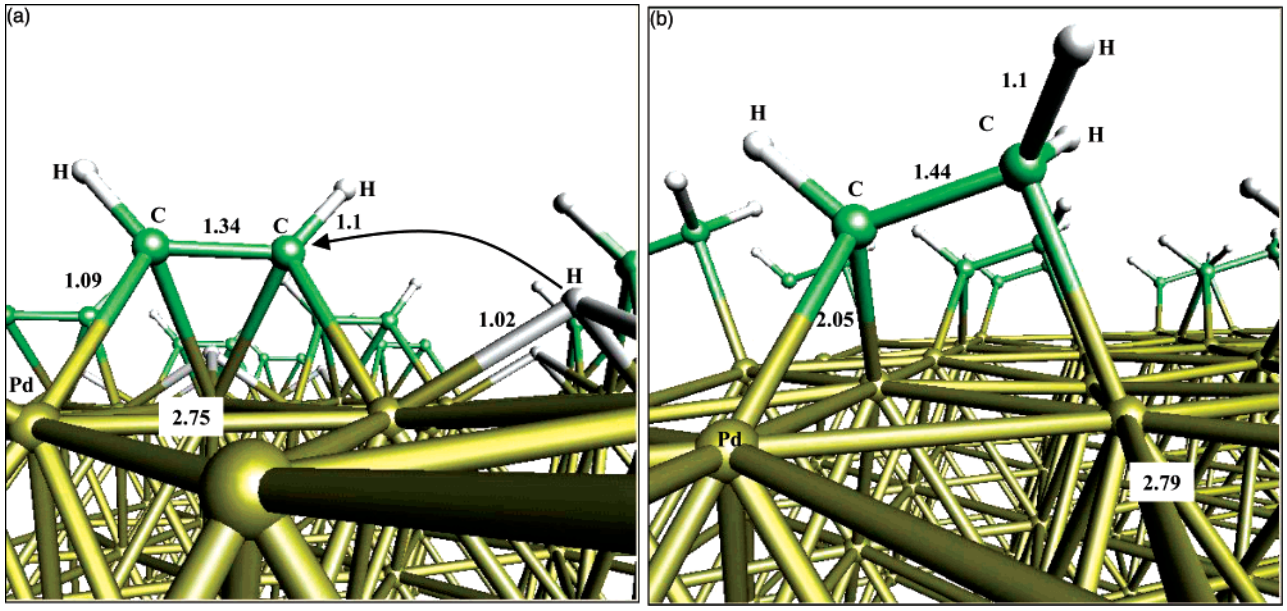

Figure 1. (a) The structure of the reactant state for acetylene hydrogenation: acetylene and hydrogen coadsorbed on Pd(111) at 25% hydrocarbon and 25% hydrogen coverage. (b) The structure of the product state for acetylene hydrogenation: vinyl adsorbed in the $\eta_1-\eta_2$ mode over Pd(111).

the energies necessary to go from 0 K to the specified reference temperature. It must also be noted, however, that for comparisons on a *relative* scale, these estimates of the reaction energies and binding energies are accurate.

Results and Discussion

Acetylene Hydrogenation to Vinyl over Pd(111). The adsorption energies and the corresponding adsorption geometries of acetylene, hydrogen, and vinyl were examined at different sites on the Pd(111) surface to find those that are most favorable. Under UHV conditions acetylene binds to the 3-fold hollow sites on Pd(111).[24,25] We calculate an adsorption energy for acetylene at this site to be −172 kJ/mol for a 2 × 2 adlayer. Acetylene bound to the Pd−Pd bridge site, however, was found to be −137 kJ/mol, which is 35 kJ/mol weaker than that for acetylene at the fcc site. Acetylene adsorbed π-bound atop a single Pd atom is even more weakly bound at −55 kJ/mol.

The C−C bond length of acetylene increases from 1.21 Å in the gas phase to 1.34 Å when acetylene adsorbs at the fcc site as seen in Figure 1a. This increase in bond length is indicative of a change in the bond order and bond character between the carbon atoms. These changes in the bond lengths are in very good agreement with the previous results reported by Pacchioni et al.[40] where the C−C bond length changes by 0.14 Å. The C atoms in acetylene rehybridize from an sp to an sp^2 configuration upon its adsorption on Pd. The C−C bond takes on more double bond character whereby each C atom interacts with two Pd atoms. The C−H bonds in this structure are distorted out of the initial plane of the molecule where the hydrogen atoms tilt away from the surface. The C−H bond lengths were calculated to be 1.1 Å.

Di-hydrogen on the other hand dissociatively adsorbs over Pd(111) at the 3-fold hollow site.[55] The resulting hydrogen atoms prefer the 3-fold fcc sites on Pd(111). The binding energy for atomic hydrogen on Pd was found to be −260 kJ/mol. This surface hydrogen atom can then react with a neighboring acetylene species to form a surface vinyl intermediate. The vinyl intermediate was therefore optimized over Pd(111) to establish its most favorable adsorption site and corresponding adsorption energy. Vinyl binds most favorably in the $\eta 1-\eta 2$ mode across the 3-fold hollow fcc site[1] (Figure 1b). We calculate an adsorption energy of −274 kJ/mol for vinyl in a 2 × 2 adlayer over Pd. The calculated C−C bond length for adsorbed vinyl is 1.50 Å, which indicates that is takes on more single bond character whereby the carbon atoms shift from sp^2 to sp^3 hybridization. Accordingly, the CH_2 carbon atom interacts with only one Pd atom while the other CH carbon atom interacts with two Pd atoms to conserve an overall sp^3 bond character. The C−H bonds again all have the same length of 1.1 Å.

The reaction energy for acetylene hydrogenation to vinyl was calculated in two ways as was described above in the Conventions section. The first involves the adsorption energies of the reactants and products and the reaction energy for acetylene hydrogenation in the ideal gas phase (no metal surface), which is computed to be −162 kJ/mol. The overall reaction energy for acetylene hydrogenation was calculated using the Haber cycle (Scheme 3) to be exothermic at −3 kJ/mol. This is an ideal reaction energy that does not consider the effect of lateral interactions between adsorbates on the surface. To account for these effects, we calculate the reaction energy to go directly from reactants to products wherein both acetylene and hydrogen are coadsorbed to Pd(111) at adjacent 3-fold hollow sites. The reactant and product states are shown in Figure 1. The difference in the energies between the optimized reactant (Figure 1a) and the product (Figure 1b) state gives an energy of reaction of −26 kJ/mol. The coadsorption of acetylene and hydrogen weaken the Pd−C and the Pd−H bonds owing to repulsive interactions between the two coadsorbed reactants. The reactant state is therefore higher in energy as compared to the product state, and the overall reaction energy therefore becomes more favorable. This change of −23 (−26- (−3)) kJ/mol is a measure of the lateral interaction effects on the hydrogenation of acetylene to vinyl at 25% hydrocarbon coverage.

The intrinsic activation barrier for acetylene hydrogenation to vinyl was calculated by using the nudged elastic band approach developed to isolate the transition state. This intrinsic activation barrier is computed to be +66 kJ/mol, which is the difference in energy between the reactant state and the transition state where acetylene and hydrogen sit at adjacent 3-fold sites. Figure 2 illustrates the path in going from the reactant to the

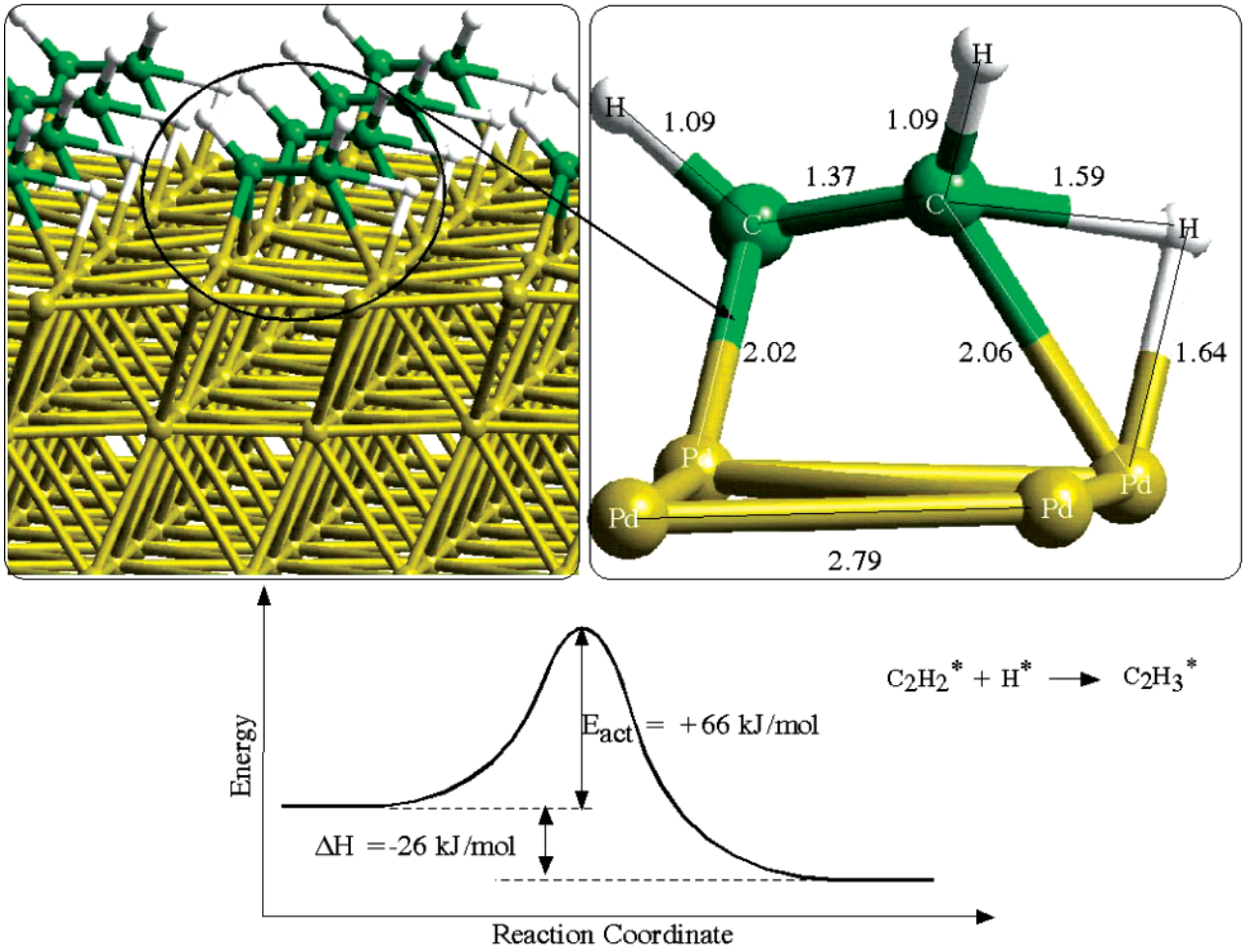

Figure 2. The transition-state structure for the hydrogenation of acetylene to vinyl over Pd(111) at 25% hydrocarbon coverage. The DFT calculated energetics along the reaction path for the hydrogenation of acetylene to vinyl is shown in the inset.

product state. The reaction involves the formation of a three-center (Pd−C−H) transition-state structure as surface hydrogen inserts into the Pd−C bond. The structure of the transition state is very similar to those found for ethylene hydrogenation[1] and other olefins.[56] The main changes along the reaction coordinate appear to be along the C−H stretch mode (involved in the bond formation).

The C−H distance in this transition state decreases from 2.7 to 1.6 Å while the Pd−H bond length increases from 1.02 to 1.8 Å. The Pd−C bond length increases from 1.8 to 2.1 Å, which indicates that there is a weakening Pd−C bond.

Coverage Effects on the Acetylene Hydrogenation Reaction. To begin to understand the effect of coverage on acetylene hydrogenation, the same reaction path was examined at 33% coverage of acetylene and 33% coverage of hydrogen. This was done by using a $\sqrt{3} \times \sqrt{3}$ super-cell (see Figure 3) The most favorable adsorption sites remain the same for all the species. The adsorption energies, however, all decreased due to repulsive interactions between neighboring adsorbates (see Table 1). The adsorption energy of acetylene and vinyl decreased by 36 and 39 kJ/mol, respectively, whereas hydrogen's adsorption energy decreased by only 12 kJ/mol. The reaction energy for this system was calculated to be −43 kJ/mol. This is 17 kJ/mol more exothermic than the reaction energy for the 2 × 2 system which included lateral interactions between coadsorbates. This increase in exothermicity is due to the increased repulsive interactions that take place at higher coverages. The binding energy of acetylene and hydrogen are weakened moreso by the increased repulsive interactions than the vinyl product state. The repulsive interactions weaken the Pd−C and Pd−H bonds which helps to facilitate the reaction between acetylene and hydrogen. The overall reaction energy therefore becomes more exothermic and favorable.

According to the Evans-Polanyi relationship,[55] the activation energy should be reduced to be proportional to the change in the overall reaction energy. We therefore expect a lower activation barrier for the $\sqrt{3} \times \sqrt{3}$ case than for the 2 × 2 case. On calculating this transition state, we find that while there are little structural changes in the transition state, the intrinsic barrier is lowered by 16 kJ/mol to +50 kJ/mol. The transition-state structure involves a three-center complex that is very similar to that found for the 2 × 2 unit cell. The C−H bond length is now 1.67 Å and the Pd−H bond length increases to 1.70 Å (Figure 4). The C−C bond length is 1.35 Å, which indicates that it has double bond character.

Vinyl Hydrogenation to Ethylene. The subsequent hydrogenation of vinyl to ethylene involves the insertion of hydrogen into the Pd−C bond of vinyl. At 25% surface coverage, vinyl adsorbs most favorably in the $\eta 1-\eta 2$ mode with a binding energy of −274 kJ/mol. Ethylene adsorbs most favorably in the di-σ adsorption mode[1,42] with an adsorption energy of −82 kJ/mol. The overall reaction energy for vinyl hydrogenation in the absence of lateral interactions is calculated according to the ideal Haber cycle in Scheme 3 to be −42 kJ/mol. On considering the coadsorption of vinyl and hydrogen at adjacent sites, however, the reaction energy is expectedly more exothermic at

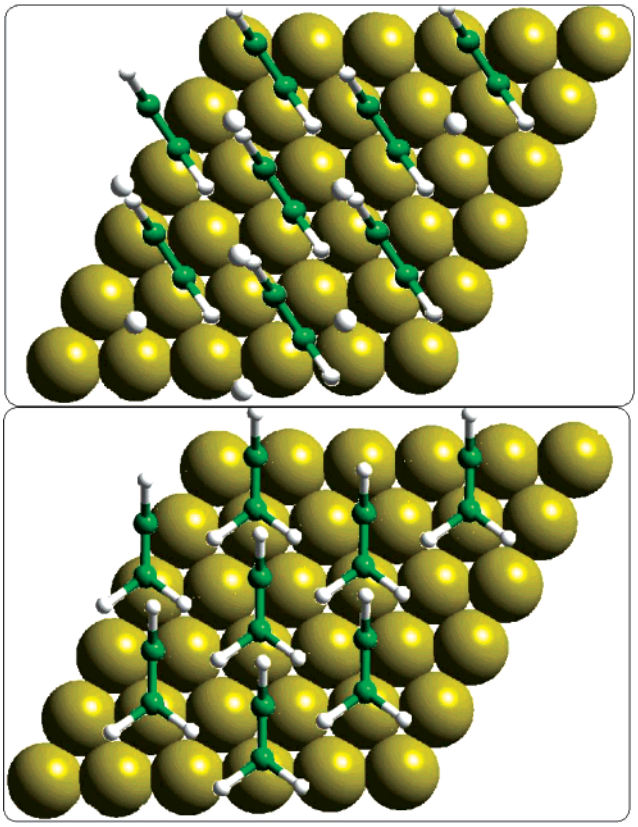

Figure 3. (a) Top view of acetylene + hydrogen adsorbed in a $\sqrt{3} \times \sqrt{3}$ ordered phase over Pd(111) at adjacent hollow sites. (b) Top view of vinyl adsorbed in a $\sqrt{3} \times \sqrt{3}$ ordered phase over Pd-(111). Vinyl adsorbs most favorably in the $\eta_1-\eta_2$ mode.

TABLE 1: Binding Energies of the Adsorbates on Pd(111) at Different Coverages (These values are calculated using eq 1 in the paper.)

species	2 × 2 unit cell (25% coverage) kJ/mol	$\sqrt{3} \times \sqrt{3}$ unit cell (33.33% coverage) kJ/mol
acetylene	−172	−136
vinyl	−274	−235
hydrogen	−260	−248
ethylene	−82	−62

−58 kJ/mol due to the increased repulsive interactions and metal atom sharing in the reactant state. The intrinsic activation barrier for vinyl hydrogenation at 25% hydrocarbon coverage is calculated using the nudged elastic band method to be +85 kJ/mol. Figure 5 shows the corresponding transition-state complex for vinyl hydrogenation to ethylene. This structure also involves a three-centered C−Pd−H complex wherein the C−C bond is oriented directly over the bridge site of palladium. The C−C bond length is now 1.43 Å, which is right between the typical C−C single bond and C−C double bond. The C−H distance decreases from 1.88 Å in the reactant state to 1.7 Å in the product state and the Pd−H bond length decreases to 1.68 Å. This structure is similar to that reported by Pallassana and Neurock[1] for the same reaction at 33% coverage. They computed the overall reaction energy and the activation barrier for vinyl hydrogenation to be −73 kJ/mol and +78 kJ/mol, respectively. These differences in the energetics for vinyl hydrogenation to ethylene at 25% and 33% hydrocarbon coverage can again be explained by lateral interactions. At the higher (33%) coverage there is a weakening of the Pd−C and Pd−H bonds in the

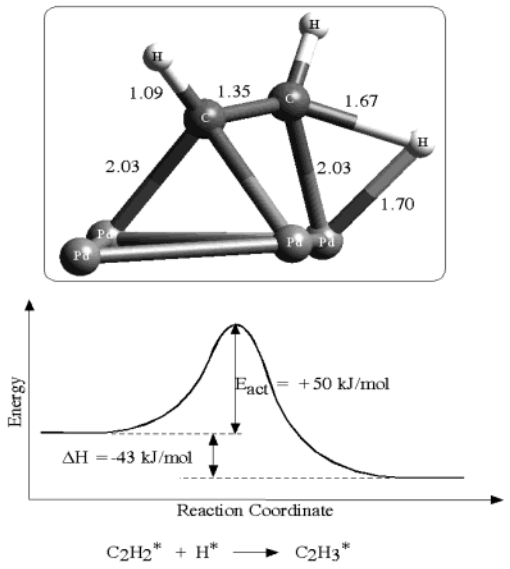

Figure 4. The transition state structure for the hydrogenation of acetylene to vinyl over Pd(111) at 33% hydrocarbon coverage. The DFT calculated energetics along the reaction path for the hydrogenation of acetylene to vinyl is shown in the inset.

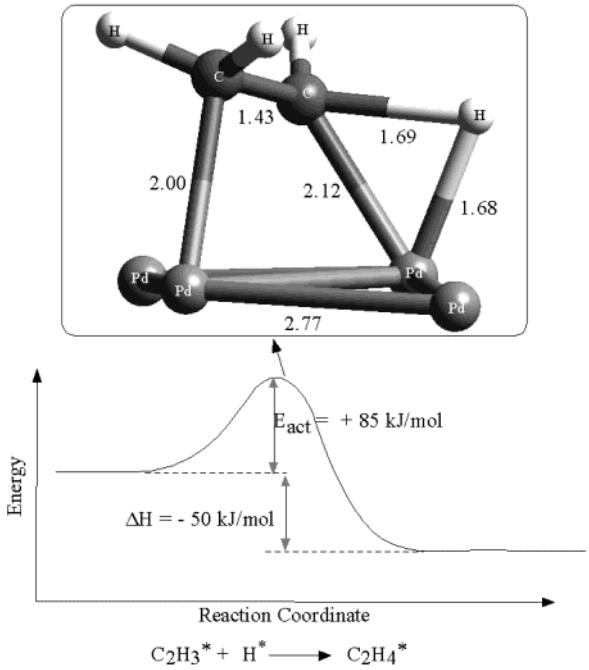

Figure 5. The transition state complex for the hydrogenation of the vinyl intermediate to ethylene over Pd(111) at 25% hydrocarbon coverage. The DFT calculated energetics along the reaction path for the hydrogenation of vinyl to ethylene is shown in the inset.

reactant state due to lateral interactions. The weaker metal−adsorbate bonds lead to a lowering of the activation barrier.[55]

Overall Hydrogenation of Acetylene to Ethylene. The reaction energies and activation barriers for acetylene hydrogenation to vinyl and vinyl hydrogenation to ethylene are given in Table 2. These results can be combined to construct an overall energy diagram for the hydrogenation of acetylene to ethylene (Figure 6a). This energy diagram can also be extended to include the hydrogenation of ethylene to ethane by including results from our previous work on ethylene hydrogenation (Figure 6b).[46] At surface hydrocarbon coverages of 25%, the reaction energy for acetylene hydrogenation to vinyl is 32 kJ/mol less exothermic than that for vinyl hydrogenation. The barrier for acetylene

TABLE 2: Overall Reaction Energies and Activation Barriers for Acetylene Hydrogenation to Ethylene through Vinyl Intermediate

reaction	acetylene + H = vinyl		vinyl + H = ethylene	
surface coverage	25%	33%	25%	33%
reaction energy (kJ/mol)	−26	−43	−58	−73
activation barrier (kJ/mol)	+66	+50	+85	+78

hydrogenation, however, is 19 kJ/mol lower than the barrier for vinyl hydrogenation at the same 25% hydrocarbon coverage. The same trend is followed at 33% hydrocarbon coverage with the reaction energy for acetylene hydrogenation being 30 kJ/mol less exothermic than the vinyl hydrogenation reaction energy (Table 2). The intrinsic activation barrier for acetylene hydrogenation is now lower by 28 kJ/mol than the intrinsic barrier for vinyl hydrogenation.

These differences in the activation energies for acetylene and vinyl hydrogenation are not very large. If we assume similar Arrhenius prefactors, the rate constants for these steps are expected to be comparable with perhaps a faster rate for the first step of acetylene hydrogenation. The results of recent TPD experiments over Pd(111) single crystals, however, suggest that the rate of vinyl hydrogenation is faster (smaller activation barrier) than acetylene hydrogenation.[37] The suggestion is based on the fact that ethylene is observed to desorb at a higher temperature of 245 K when acetylene and hydrogen are reacted over Pd(111) than when vinyl iodide and hydrogen are heated over Pd(111). The vinyl iodide bond breaks quite easily at low temperatures, leaving the surface populated with vinyl intermediates. The lower temperature ethylene desorption peak (175 K) in this case indicates that vinyl is more reactive than acetylene. These experiments, however, were carried out at higher exposures which were 1.2−1.7 L. The same work also reported that at the lower exposures of 0.3 L, the ethylene desorption temperature increased to 245 K.[37] This increase in temperature was suggested to be due to vinyl hydrogenation. As this is also the temperature for ethylene desorption due to acetylene hydrogenation, it suggests that that the activation barriers for both acetylene and vinyl hydrogenation should be essentially the same at low exposures. Furthermore, based on intensities of TPD results of vinyl iodide at different exposures[37] it is also clear that increasing exposure leads to increasing monolayer surface coverage of vinyl iodide. This is thus in good agreement with our theoretical results which also indicate similar intrinsic activation barriers and rate constants for both acetylene hydrogenation and vinyl hydrogenation at the low hydrocarbon coverage of 0.25−0.33 ML.

At higher exposures however, it is seen from experimental results that acetylene hydrogenation becomes rate limiting, presumably due to changes in the coverage of the surface intermediates. This therefore suggests that coverage effects can significantly influence the relative hydrogenation rates of acetylene and vinyl. This could be due to the different local environment around the reactants at higher coverages, which change the relative kinetics of acetylene and vinyl hydrogenation. It could also be due to a shift in the acetylene and vinyl adsorption modes at higher coverages from their most favorable sites, leading to a change of the reaction pathways of the hydrogenation. It is therefore clear that coverage effects play an important role in the reaction kinetics and should be included in the development of kinetic models in order to provide a more realistic representation of the kinetics.

We have recently applied such lateral interaction models to account for these effects along with the elementary reaction

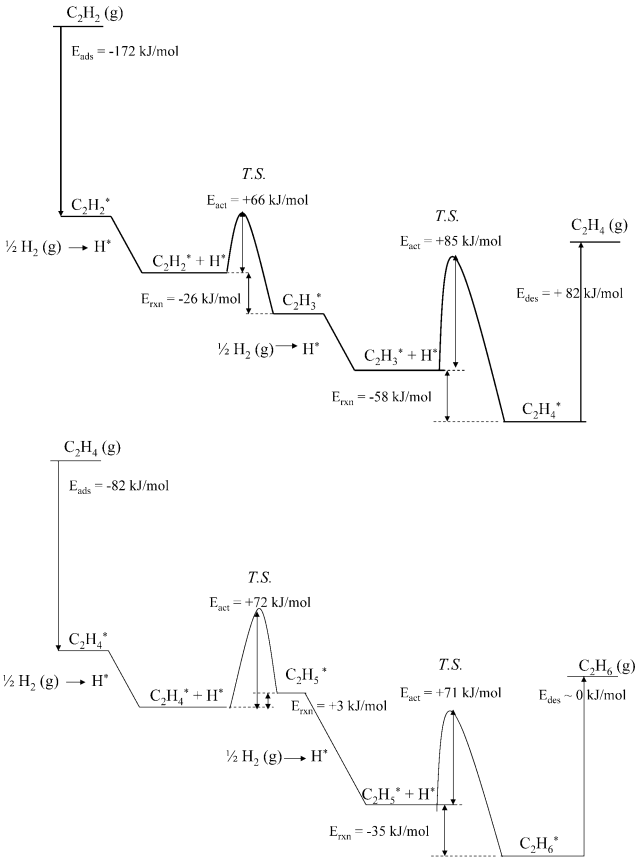

Figure 6. The overall reaction energies for a sequence of elementary steps that comprise the postulated catalytic cycle for acetylene hydrogenation to ethylene at 25% hydrocarbon surface coverage.

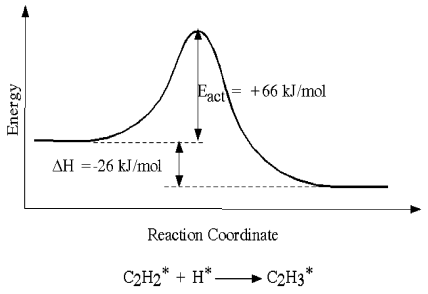

Figure 7. The DFT calculated energetics along the reaction path for the hydrogenation of acetylene to vinyl in the presence of tetrahedral subsurface hydrogen.

energetics in a kinetic Monte Carlo simulation algorithm[57] to examine the hydrogenation of acetylene. The resulting turnover frequencies and general kinetic behavior are in very good agreement with the reported experimental results.[58]

Effect of Subsurface Hydrogen. We have assumed in this work that these reactions occur over a clean Pd(111) surface. It is well-known, however, that hydrogen can diffuse into Pd, leading to subsurface hydrogen and hydride formation.[59] At higher temperatures, the preadsorption of hydrogen was reported to increase the sticking probability of acetylene.[30] This increase in the sticking probability was thought to be due to the effects of subsurface hydrogen. To study the influence of subsurface hydrogen on acetylene hydrogenation kinetics, we repeated the calculations for acetylene hydrogenation to vinyl in the presence of a quarter monolayer of subsurface hydrogen (see Figure 7) This corresponds to an overall composition of $PdH_{0.08}$, which is close to the α-hydride phase for Pd.[59] These calculations

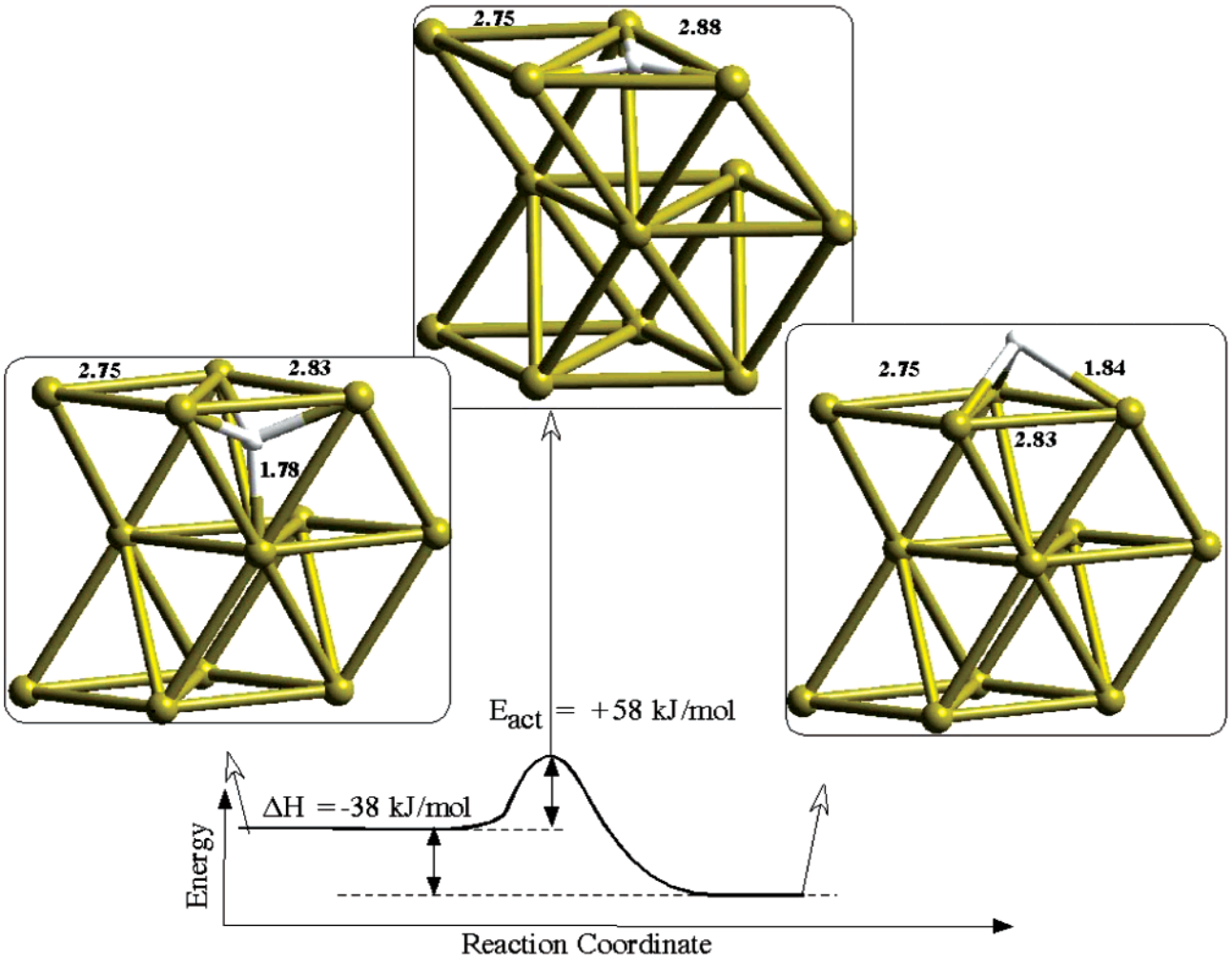

Figure 8. The reaction path for subsurface hydrogen bound at a tetrahedral site to diffusion to the surface of Pd(111).

TABLE 3: Binding Energies of the Adsorbates on Pd(111) with and without Subsurface Hydrogen[a] in the System[b]

species	without subsurface hydrogen kJ/mol	with subsurface hydrogen kJ/mol
acetylene	−172	−161
vinyl	−274	−266
hydrogen	−260	−261

[a] 1/4 monolayer of subsurface hydrogen in the system. [b] These calculations are for a 2 × 2 unit cell, and the energies are computed using eq 1 in the paper.

showed that the adsorption energies of acetylene and vinyl decreased by 11 and 8 kJ/mol, respectively (see Table 3). The reaction energy and the activation barrier, however, were unchanged. This suggests that the presence of subsurface hydrogen affects both the reactant and product states nearly the same. Therefore there is essentially no change in the calculated reaction energetics. The *indirect* influence of subsurface hydrogen is very small in that there is practically no change in the reaction energetics for acetylene hydrogenation. We also expect to see similar results for higher coverages of subsurface hydrogen (β-hydride phase).

On the basis of HREELS experiments, Ceyer et al.[60] indicate that subsurface hydrogen can be *directly* involved in the hydrogenation of acetylene to ethylene on Ni(111). Both Sautet et al.[61] and Michaelides et al.[62] have reported on the reaction energies and activation barriers for subsurface hydrogen that is *directly* involved in the hydrogenation of methyl over Ni(111). To verify a similar possibility in this case, it was decided to examine first the kinetics for diffusion of subsurface hydrogen to the surface to form chemisorbed hydrogen. The diffusion path studied here is mapped out in Figure 8. The reactant state was optimized with hydrogen in the tetrahedral subsurface site. The product site consisted of hydrogen chemisorbed over the hcp hollow site. The overall energy for diffusion was exothermic at −38 kJ/mol. The activation barrier for diffusion was calculated to be +58 kJ/mol. The transition-state structure shown in Figure 8 is one in which the emerging hydrogen atom sits slightly below the plane of the Pd surface layer. There is an expansion in the Pd−Pd bonds from 2.83 to 2.88 Å to accommodate the emerging hydrogen. The overall energy and the activation barrier for subsurface hydrogen to diffuse to the surface is thus comparable to that for acetylene hydrogenation to vinyl. Subsurface hydrogen could potentially be involved in the hydrogenation. We suspect, however, that hydrogen is equilibrated with the surface under actual conditions whereby there is a substantial background partial pressure of hydrogen and that the acetylene reacts with surface-bound hydrogen intermediates. A more complete explanation will require calculating the activation barrier for the subsurface hydrogenation step followed by a complete simulation of the full kinetics of this system, including adsorption, desorption, hydrogenation, and surface and subsurface diffusion paths.

Conclusion

The adsorption energies of acetylene, hydrogen, vinyl, and ethylene are computed to be −172 (−136), −260 (−248), −274 (−235), and −82 (−62) kJ/mol, respectively, for 25% (33%) coverage over Pd(111). The reaction energy for acetylene hydrogenation to vinyl is computed at −26 (−43) kJ/mol at 25% (33%) coverages. The reaction energy for the hydrogenation of vinyl to ethylene is computed at −58 kJ/mol and −73 kJ/mol at 25% and 33% coverages, respectively. The intrinsic activation barrier for acetylene hydrogenation to vinyl is +66 (+50) kJ/mol for 25% (33%) coverage and is comparable to the barrier for vinyl hydrogenation to ethylene (+85 kJ/mol for 25% coverage and +78 kJ/mol for 33% coverage). Although there are moderate changes in the adsorption energies of the adsorbates due to subsurface hydrogen, DFT calculations do not show any indirect effect of the presence of subsurface hydrogen on the reaction energetics and pathways for acetylene hydrogenation. The calculated activation barrier for hydrogen to diffuse from the subsurface to the surface was +58 kJ/mol which is similar to that for acetylene hydrogenation.

Acknowledgment. We kindly acknowledge The Dow Chemical Company for the financial support for this work. M.N. thanks Drs. Robert Gulotty, David West, and Istvan Lengyl from Dow for their scientific discussions. The Legion Computing group at the Computer Science Department at the University of Virginia and the NCSA supercomputing center at Illinois are also acknowledged for computing resources. Helpful discussions with Sanket K. Desai, Dr. Qingfeng Ge, and Dr. Michael Palmer are also acknowledged.

References and Notes

(1) Pallassana, V.; Neurock, M. *J.Catalysis* **2000**, *191*, 301−317.
(2) Zhang, Q.; Li, J.; Liu, X.; Zhu, Q. *Appl. Catal. A: General* **2000**, *197*, 221−228.
(3) Canh, N. T.; Blaise, D.; Patrick, S.; Charles, C. Selective Hydrogenation Catalyst and a Process using that Catalyst. In *U.S. Patent & Trademark Office*; Institut Francais du Petrole: France, 2000.
(4) Coq, B.; Figueras, F. *J. Mol. Catal. A: Chemical* **2001**, *173*, 117−134.
(5) Brown, M. W.; Penlidis, A.; Sullivan, G. *Can. J. Chem. Eng.* **1991**, *69*, 152−164.
(6) Bos, A. N. R.; Westerterp, K. R. *Chem. Eng. Process.* **1993**, *32*, pp 1−7.
(7) Horuiti, J.; Polanyi, M. *Trans. Faraday Soc.* **1934**, *30*, 1164.
(8) Bond, G. C.; Wells, P. B. *J. Catal.* **1965**, *4*, 211.
(9) Bond, G. C.; Wells, P. B. *J. Catal.* **1966**, *5*, 65.
(10) Bond, G. C.; Wells, P. B. *J. Catal.* **1966**, *5*, 419.
(11) *Advances in Catalysis and Related Subjects*; Eley, D. D., Pines, H., Weisz, P. B., Eds.; Academic Press: New York and London, 1964; Vol. 15.
(12) Bond, G. C.; Wells, P. B. *J. Catal.* **1966**, *6*, 397−410.
(13) Arnett, R. L.; Crawford, B. L. *J. Chem. Phys.* **1950**, *18*, 118.
(14) Margitfalvi, J.; Guczi, L.; Weiss, A. H. *React. Kinet. Catal. Lett.* **1980**, *15*, 475−479.
(15) Bond, G. C. *Catalysis by Metals*; Academic Press: London, 1962.
(16) McGown, W. T.; Kemball, C.; Whan, D. *J. Catal.* **1978**, *51*, 173−184.
(17) Moses, J. M.; Weiss, A. H.; Matusek, K.; Guczi, L. The Effect of Pd Dispersion in Acetylene Selective Hydrogenation. *Proc. 8th Int. Congr. Catal. Dechema*, 1984, Berlin.
(18) Cider, L.; Schoon, N.-H. *Ind. Eng. Chem. Res.* **1991**, *30*, 1437−1443.
(19) Borodzinski, A.; Golebiowski, A. *Langmuir* **1997**, *13*, 883−887.
(20) Borodzinski, A.; Cybulski, A. *Appl. Catal. A: General* **2000**, *198*, 51−66.
(21) Asad, S.; Al-Ammar; Webb, G. *J. Phys. Chem.* **1978**, *1*, 195−205.
(22) Bos, A. N. R.; Bootsma, E. S.; Foeth, F.; Sleyster, H. W. J.; Westerterp, K. R. *Chem. Eng. Process.* **1993**, *32*, 53−63.
(23) Janssens, T. V. W.; Volkening, S.; Zambelli, T.; Wintterlin, J. *J. Phys. Chem. B* **1998**, *102*, 6521−6528.
(24) Dunphy, J. C.; Rose, M.; Behler, S.; Ogletree, D. F.; Salmeron, M. *Phys. Rev. B* **1998**, *57*, R12707.
(25) Sellars, H. *J. Phys. Chem.* **1990**, *94*, 8329−8333.
(26) Clotet, A.; Pacchioni, G. *Surf. Sci.* **1996**, *346*, 91−107.
(27) Fahmi, A.; Santen, R. A. V. *Surf. Sci.* **1997**, *371*, 53−62.
(28) Hoffmann, R. *Rev. Mod. Phys.* **1988**, *60*, 601−628.
(29) Shriver, D.; Atkins, P. *Inorganic Chemistry*, 3rd ed.; W. H. Freeman and Company: New York, 1999.
(30) Sandell, A.; Beutler, A.; Jaworowski, A.; Wiklund, M.; Heister, K.; Nyholm, R.; Andersen, J. N. *Surf. Sci.* **1998**, *415*, 411−422.
(31) Guo, X. C.; Madix, R. *J. Catal.* **1995**, *155*, 336−344.
(32) Tysoe, W. T.; Nyberg, G. L.; Lambert, R. M. *Surf. Sci.* **1983**, *135*, 128−146.
(33) Kesmodal, L. L.; Waddill, G. D.; Gates, J. A. *Surf. Sci.* **1983**, *138*, 464−474.
(34) Tysoe, W. T.; Nyberg, G. L.; Lambert, R. M. *J. Phys. Chem.* **1986**, *90*, 3188−3192.
(35) Gates, J. A.; Kesmodal, L. L. *Surf. Sci.* **1983**, *124*, 68−86.
(36) Clotet, A.; Ricart, J. M.; Pacchioni, G. *J. Mol. Struct. (THEOCHEM)* **1999**, *458*, 123−129.
(37) Azad, S.; Kaltchev, M.; Stacchiola, D.; Wu, G.; Tysoe, W. T. *J. Phys. Chem. B* **2000**, *104*, 3107−3115.
(38) Ormerod, R. M.; Lambert, R. M.; Hoffmann, H.; Zaera, F.; Wang, L. P.; Bennett, D. W.; Tysoe, W. T. *J. Phys. Chem.* **1994**, *98*, 2134−2138.
(39) Kaltchev, M.; Stacchiola, D.; Molero, H.; Wu, G.; Blumenfeld, A.; Tysoe, W. T. *Catal. Lett.* **1999**, *60*, 11−14.
(40) Pacchioni, G.; Lambert, R. M. *Surf. Sci.* **1994**, *304*, 208−222.
(41) Bent, B. E. *Chem. Rev.* **1996**, *96*, 1361−1390.
(42) Neurock, M.; Santen, R. A. v. *J. Phys. Chem. B* **2000**, *104*, 11127−11145.
(43) Hoffmann, R.; Silvestre, J. *Langmiur* **1985**, *1*, 621.
(44) Sautet, P.; Paul, J. *J. Am. Chem. Soc.* **1991**, *9*, 245−260.
(45) Anderson, A. B.; Choe, S. J. *J. Phys. Chem.* **1989**, *93*, 6145−6149.
(46) Nakatsuji, H.; Hada, M.; Yonezawa, T. *Surf. Sci.* **1987**, *185*, 319−342.
(47) Payne, M. C.; Teter, M. P.; Allan, D. C.; Arias, T. A.; Joannopoulos, J. D. *Rev. Mod. Phys.* **1992**, *64*, 1045.
(48) Head-Gordon, M. *J. Phys. Chem.* **1996**, *100*, 13213−13225.
(49) Zeigler, T. *Chem. Rev.* **1991**, *91*, 651.
(50) Kresse, G.; Furthmuller, J. *Phys. Rev. B* **1996**, *54* (11), 169−186.
(51) Kresse, G.; Hafner, J. *J. Phys.: Condens. Matter* **1994**, *6*, 8245.
(52) Perdew, J. P.; Chevary, J. A.; Vosto, S. H.; Jackson, K. A.; Pederson, M. R.; Singh, D. J.; Frolhais, C. *Phys. Rev. B* **1992**, *46*, 6671.
(53) Mills, G.; Jonsson, H.; Schenter, G. K. *Surf. Sci.* **1995**, *324*, 305−337.
(54) Steinfeld, J. I.; Francisco, J. S.; Hase, W. L. *Chemical Kinetics and Dynamics*; Prentice Hall: New Jersey, 1989.
(55) Gates, B. C. *Catalytic Chemistry*; John Wiley and Sons Inc.: New York, 1992.
(56) Neurock, M.; Pallassana, V. Modeling Transition States for Selective Catalytic Hydrogenation Paths on Transition Metal Surfaces; ACS Symposium Series 721, 1998, Dallas, Texas.
(57) Hansen, E. *Methodology for Stochastic Simulations of Surface Kinetics from First-Principles*; University of Virginia, 2000.
(58) Mei, D.; Sheth, P.; Hansen, E.; Neurock, M. To be submitted.
(59) *Metal Hydrides*; Mueller, W. M., Blackedge, J. P., Libowitz, G. G., Eds.; Academic Press Inc: New York, 1968.
(60) Haug, K. L.; Burgi, T.; Trautman, T. R.; Ceyer, S. T. *J. Am. Chem. Soc.* **1998**, *120*, 8885−8886.
(61) Ledentu, V.; Dong, W.; Sautet, P. *J. Am. Chem. Soc.* **2000**, *122*, 1796−1801.
(62) Michaelides, A.; Hu, P.; Alavi, A. *J. Chem. Phys.* **1999**, *111*, 1343−1345.